Completion of each coupling was checked by a chloranil color test.[82] Threonine was used without benzyl ether protection; possible branching peptides (Boc-D-Trp-Lys-$NHNH_2$) have been eliminated by purification on Sephadex LH20 after cleavage from the resin via hydrazinolysis. The linear Boc protected hexapeptide hydrazides were shown to be homogenous by TLC chromatography and gave the expected amino acid analysis values and reasonable NMR spectra. After deprotection they were cyclized without further purification in high dilution (10^{-3} mmol L^{-1}). Usual workup and purification on Sephadex LH20 or HPLC gave the desired compounds. Satisfactory amino acid analysis was obtained.

Acknowledgment. O.W.S. is supported by the Danish Natural Science Research Council (J.nr. 11-3294). H. Kogler thanks the Studienstiftung des Deutschen Volkes and the Fonds der Chemischen Industrie. J.Z. acknowledges the Hermann-Schlosser-Stiftung for a grant. We thank the Deutsche Forschungsgemeinschaft and the Fonds der Chemischen Industrie for financial support. We also acknowledge the Hoechst AG and Degussa for support.

Registry No. 1, 87308-19-8; **2**, 87282-39-1; **3**, 77236-35-2.

(82) Christensen, Th. *Acta Chem. Scand.* **1979**, *33*, 763.
(83) Bystrov, V. *Prog. Nucl. Magn. Reson. Spectrosc.* **1976**, *10*, 41.

Kinetics of the Scrambling Reaction between Dimanganese and Dirhenium Decacarbonyl

Antonio Marcomini and Anthony Poë*

Contribution from the Department of Chemistry and Erindale College, University of Toronto, Mississauga, Ontario, Canada L5L 1C6. *Received December 28, 1982*

Abstract: The scrambling reaction between $Mn_2(CO)_{10}$ and $Re_2(CO)_{10}$ to form $MnRe(CO)_{10}$ proceeds cleanly to a stable equilibrium in decalin at 170–190 °C. Studies of the initial rates show that two paths are followed, the major one being evident over the whole range of temperatures and partial pressures of CO above the solutions. The kinetics suggest that it involves prior aggregation to form $Mn_2Re_2(CO)_{20}$ which undergoes stepwise loss of CO to form the clusters $Mn_2Re_2(CO)_{20-n}$ ($n \leq 4$). All these clusters can be envisaged to be quasitetrahedral and to contain one Mn–Mn and one Re–Re bond together with n Mn–Re bonds and $4 - n$ Mn(μ-CO)Re bonds. When the requisite number of CO ligands have been removed the Mn–Mn and Re–Re bonds are lost, either by CO insertion or by redistribution of the M–M and M(μ-CO)M bonds within the cluster. Further CO insertion leads to $Mn_2Re_2(CO)_{20}$ containing two Mn–Re bonds, and this readily fragments to form $MnRe(CO)_{10}$. At low partial pressures of CO the rate-determining step is the formation of $Mn_2Re_2(CO)_{20}$ or $Mn_2Re_2(CO)_{19}$ and the activation parameters are $\Delta H^{\ddagger} = 22 \pm 3$ kcal mol^{-1} and $\Delta S^{\ddagger} = -20 \pm 6$ cal K^{-1} mol^{-1}. The other path is most evident at 190 °C under small partial pressures of CO, and it appears to involve prior loss of CO from the decacarbonyls before aggregation. The kinetics suggest that scrambling occurs mainly via the tetranuclear intermediate $Mn_2Re_2(CO)_{16}$.

It has recently been shown[1] that the scrambling reaction in eq 1 does not occur in decalin under an atmosphere of carbon monoxide at 130–140 °C and that it occurs only very slowly in the absence of CO. This is clear evidence that at least two of

$$Mn_2(CO)_{10} + Re_2(CO)_{10} \rightleftharpoons 2MnRe(CO)_{10} \quad (1)$$

the complexes involved are not undergoing homolytic fission under these conditions as had been proposed.[2,3] Studies of the isotopic scrambling reaction in eq 2 show that it does not occur in *n*-octane

$$^{185}Re_2(CO)_{10} + {}^{187}Re_2(CO)_{10} \rightleftharpoons 2{}^{185}Re{}^{187}Re(CO)_{10} \quad (2)$$

at 150 °C under CO although it is complete after 14 h under argon.[4] While these results show that CO dissociation must play an essential role in the scrambling process they do not provide any evidence for the detailed mechanism of the reactions. We report here some quite extensive kinetic studies of reaction 1 that provide a clear indication of the probable mechanism.

Experimental Section

$Mn_2(CO)_{10}$ (Strem Chemicals) and $Re_2(CO)_{10}$ (Alpha Inorganics) were used as received. Decalin (Aldrich) was purified by successive distillations under reduced pressure until the absorption maxima at 268 and 274 nm due to tetralin were reduced to a negligible value (see Results section). It was stored over molecular sieves. Reactions were carried out in Schlenk tubes fitted with rubber septum caps and immersed in an oil bath (Lauda Model WB-20) maintained to within ±0.1 °C. Oxygen was removed by multiple freeze–pump–thaw cycles under vacuum, and atmospheres of N_2 (Canox Ltd.), CO (Matheson Canada Ltd.), or CO–N_2 mixtures of known composition (Matheson Canada Ltd.) were maintained above the solutions during the reactions. Samples were removed by means of a syringe fitted with a stainless steel needle. IR spectra of the solutions were measured in cells with KBr windows and path lengths of 1.0 or 0.1 mm as convenient. Pye-Unicam SP3-200 or Perkin-Elmer 337 or 180 spectrophotometers were used. UV–vis spectra were measured with a Unicam SP-800 spectrophotometer.

The formation of $MnRe(CO)_{10}$ was established by reaction of $Re_2(CO)_{10}$ with a large excess of $Mn_2(CO)_{10}$. When the absorption due to $Re_2(CO)_{10}$ at 2070 cm^{-1} had been reduced to a negligible value the unreacted $Mn_2(CO)_{10}$ was removed by decomposing it under O_2 at 130 °C.[2] The product solution, after filtration, showed IR bands in the ranges 1800–2300 and 400–750 cm^{-1} that were identical with those reported for $MnRe(CO)_{10}$.[5] The UV–vis spectra of these solutions showed a maximum at 324 nm.[2] After deoxygenation, reaction with triphenylphosphine at 140 °C proceeded to form $MnRe(CO)_8(PPh_3)_2$ with a rate constant of 2.43×10^{-4} s^{-1} in excellent agreement with values obtained from separately isolated $MnRe(CO)_{10}$.[6]

Kinetics were followed by monitoring the decrease in intensity of the distinctive band due to $Re_2(CO)_{10}$ at 2070 cm^{-1}. The absorption due to this band was shown to obey Beer's law. The reaction was also accompanied by a decrease in the intensity of IR bands due to $Mn_2(CO)_{10}$ and an increase in those attributable to $MnRe(CO)_{10}$. The reaction mixtures attained equilibria after ≥30 min. The equilibrium mixtures were stable for as long as 1 h at 190 °C and equilibrium constants were estimated by measurement of the absorbance due to unreacted $Re_2(CO)_{10}$. It was shown that equilibrium could be approached from both directions. Careful attention was paid to the intensities of the bands due to $Mn_2(CO)_{10}$ and $MnRe(CO)_{10}$ so as to establish that no decomposition had occurred. This was revealed clearly in cases where deoxygenation had not been complete, or where levels of tetralin in the decalin had not been

(1) Schmidt, S. P.; Trogler, W. C.; Basolo, F. *Inorg. Chem.* **1982**, *21*, 1698.
(2) Fawcett, J. P.; Poë, A. J.; Sharma, K. R. *J. Am. Chem. Soc.* **1976**, *98*, 1401.
(3) Fawcett, J. P.; Poë, A. J.; Sharma, K. R. *J. Chem. Soc., Dalton Trans.* **1979**, 1886.
(4) Stolzenberg, A. M.; Muetterties, E. L. *J. Am. Chem. Soc.* **1983**, *105*, 822.
(5) Flitcroft, N.; Huggins, D. K.; Kaesz, H. D. *Inorg. Chem.* **1964**, *3*, 1123.
(6) Fawcett, J. P.; Poë, A. J. *J. Chem. Soc., Dalton Trans.* **1976**, 2039.

0002-7863/83/1505-6952$01.50/0

Table I. Least-Squares Parameters for Reactions at High Values of $C(Mn_2)$ and $C(Re_2)$ when $R_i{}^a = k_0 + k_2C(Mn_2)C(Re_2)$

temp, °C	$p(CO)$,[b] %	10^9k_0, M s^{-1}	10^4k_2, M^{-1} s^{-1}	$\sigma(R_i)$,[c] %
190.0	0	699 ± 132	523 ± 44	7.2
	15.3	560 ± 67	141 ± 26	
	25.0	172 ± 44	191 ± 19	
	40	97 ± 14	139 ± 9	
	71	17 ± 2	122 ± 9	
	100	−14 ± 14	105 ± 7	
180.0	25.0	36 ± 23	99.3 ± 12.0	9.6
	40	0	85.7 ± 4.1	
	71	0	53.2 ± 3.0	
	100	0	24.1 ± 1.2	
170.0	25.0	0	38.6 ± 2.1	
	40	0	33.4 ± 1.9	
	71	0	17.8 ± 1.0	
	100	0	7.2 ± 0.4	

[a] Initial rates. [b] Mole % of CO in CO–N_2 gas mixtures above reacting solutions. [c] Standard deviations of individual measurements of R_i obtained by the mehtod of pooled variances.[10]

sufficiently reduced. In these cases, attainment of an unstable equilibrium mixture was followed by a further decrease in the absorbance of bands due to $Mn_2(CO)_{10}$, a decrease in absorbances due to $MnRe(CO)_{10}$, and an increase in absorbances due to $Re_2(CO)_{10}$. This shows that instability of the $Mn_2(CO)_{10}$ was the main cause of shifts in the equilibria under these conditions. Only equilibrium data obtained in the absence of such shifts were accepted. The equilibrium constants and the values of $\Delta H°$ and $\Delta S°$ obtained from them will be reported elsewhere.[7]

Under conditions that were convenient for measurement, reactions approached equilibrium mixtures containing 30–60% of the initial concentration of $Re_2(CO)_{10}$. Since kinetics turn out to be quite complex, and a full rate expression for approach to equilibrium would be difficult to obtain, the rate data were expressed in terms of initial rates of loss of $Re_2(CO)_{10}$ measured over the first 10–15% of reaction.

Results

Reaction at 170 °C occurred at convenient rates only at relatively high concentrations of complex ($\gtrsim 5 \times 10^{-3}$ M), but at 190 °C initial concentrations could be reduced to ca. 1×10^{-3} M. Rates were found to increase with increasing initial concentration, $C(Mn_2)$, of $Mn_2(CO)_{10}$ at constant values of $C(Re_2)$ and vice versa, and good linear plots of initial rates, R_i, against $C(Mn_2)C(Re_2)$ were obtained at high concentrations. Since the rates were reduced by the presence of CO, most measurements were made under atmospheres containing a controlled and known percent, $p(CO)$, of CO in the CO–N_2 mixtures. No attempt has been made to convert $p(CO)$ values into values of [CO] in solution since the solubility of CO in decalin has only been measured up to 70 °C[8] and extrapolation to 170–190 °C would not give reliable values. Henry's law is assumed to hold so relative values of [CO] at a given temperature are determined by the relative values of $p(CO)$. Some data are shown in Figures 1 and 2 where the straight lines are those obtained from a weighted linear least-squares analysis of the dependence of R_i on $C(Mn_2)C(Re_2)$.[9] Values of the gradients and intercepts and of $\sigma(R_i)$ are shown in Table I. The

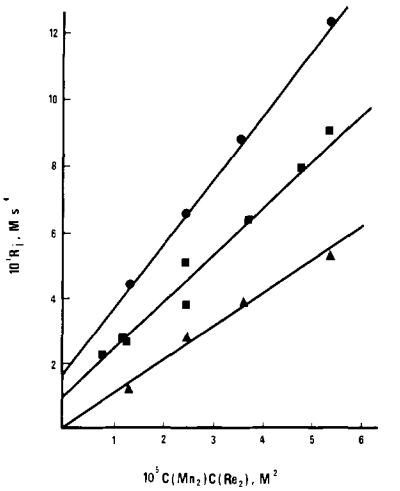

Figure 1. Examples of dependence of initial rates on $C(Mn_2)C(Re_2)$ at 190 °C under various partial pressures of CO: (●) $p(CO)$ = 25%; (■) $p(CO)$ = 40%; (▲) $p(CO)$ = 100%.

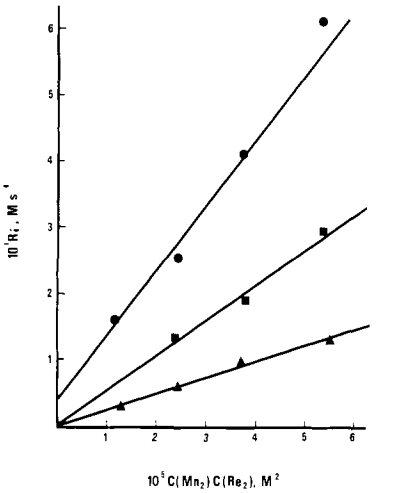

Figure 2. Examples of dependence of initial rates on $C(Mn_2)C(Re_2)$ at 180 °C under various partial pressures of CO: (●) $p(CO)$ = 25%; (■) $p(CO)$ = 70%; (▲) $p(CO)$ = 100%.

gradients are expressed as pseudo-second-order rate constants, k_2, and the intercepts as pseudo-zero-order rate constants, k_0.

The values of k_2 and k_0 are both dependent on $p(CO)$. Figure 3 shows that at 170 and 180 °C good linear plots with large intercepts are found when $1/k_2$ is plotted against $p(CO)^3$. Figure 4 shows that a plot of $1/k_2$ against $p(CO)^2$ is linear, within the experimental uncertainties, for reaction at 190 °C. However, a plot of $1/k_2$ against $p(CO)$ is also reasonably linear so that all that we can conclude is that reaction at 190 °C is less dependent on $p(CO)$ than reactions at lower temperatures. In either case the value of $1/k_2$ for reactions carried out under N_2 at 190 °C lies well below the linear plot. Only at 190 °C are enough values of k_0 available for its dependence on $p(CO)$ to be obtained. Figure 5 shows that a linear dependence of $1/k_0$ on $p(CO)^2$ is followed quite well up to $p(CO)$ = 40%, the intercept being negligible.

Some data were obtained for reactions under N_2 at 190 °C with considerably lower values of $C(Mn_2)$ and $C(Re_2)$. Rates increase individually with $C(Mn_2)$ and $C(Re_2)$, and with the product $C(Mn_2)C(Re_2)$, but the gradient of the plot of R_i against $C(Mn_2)C(Re_2)$ decreases with increasing $C(Mn_2)C(Re_2)$. Figure 6 shows a plot of R_B against $C(Mn_2)C(Re_2)$ where $R_B = R_i - k_2C(Mn_2)C(Re_2) = R_i - R_A$. The curvature suggests that a limiting rate, independent of $C(Mn_2)C(Re_2)$, is approached at high concentrations. This is supported by the plot of $1/R_B$ against $1/C(Mn_2)C(Re_2)$ shown in Figure 7. The intercept leads to a value of $(5.9 \pm 1.7) \times 10^{-7}$ M s^{-1} for the limiting rate.

(7) Marcomini, A.; Poë, A. J. *J. Chem. Soc., Dalton Trans.*, in press.
(8) Basato, M.; Fawcett, J. P.; Poë, A. J. *J. Chem. Soc., Dalton Trans.* **1974**, 1350.
(9) Each value of R_i was weighted according to the assumption of a constant percent uncertainty at a given temperature. The standard deviations of the slopes and, where appropriate, the intercepts were obtained from estimates of the uncertainty of an individual measurement. These were obtained by the method of pooled variances,[10] $\sigma(R_i)$ being expressed by $100\{\sum[(R_i(obsd) - R_i(calcd))/R_i(calcd)]^2/(N-n)\}^{1/2}$. $R_i(obsd) - R_i(calcd)$ is the difference between an individual observed value of R_i and that calculated from the least-squares gradients and intercepts at the particular value of $C(Mn_2)C(Re_2)$. N represents the total number of measurements in the set of data and n the total number of parameters being obtained from that set. This pooling had the effect of increasing the number of degrees of freedom, $N - n$, so that the estimates of $\sigma(R_i)$ are close to the true values that would have been obtained at infinitely high values of $N - n$.
(10) Mandel, J. "The Statistical Analysis of Experimental Data"; Interscience: New York, 1964; p 67.

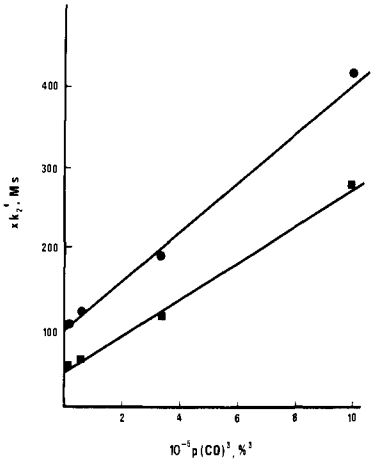

Figure 3. Dependence of x/k_2 on $p(CO)$: (●) $x = 1$, $T = 180$ °C; (■) $x = 0.2$, $T = 170$ °C.

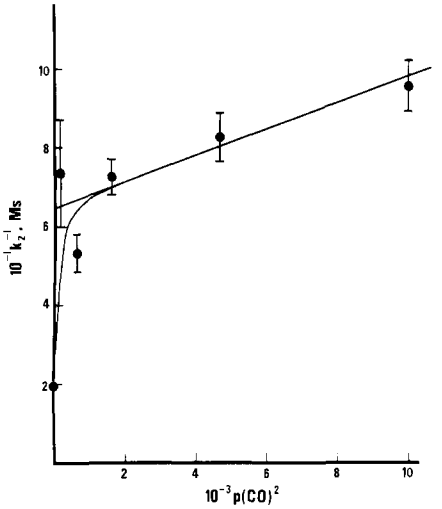

Figure 4. Dependence of $1/k_2$ on $p(CO)$ at 190 °C. Uncertainties reflect those for k_2 shown in Table I.

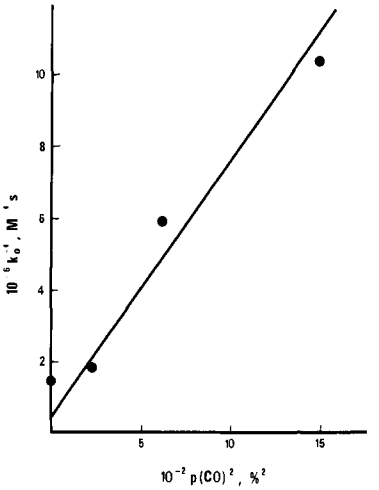

Figure 5. Dependence of $1/k_0$ on $p(CO)$ at 190 °C.

Discussion

The kinetic data for this scrambling reaction are extensive and quite complicated. They represent the first observations on such a system and we offer the following analysis as a logical and reasonable account of what is occurring.

The data in Figures 1–3 and 6 suggest that there are two kinetically distinguishable paths involved in the reaction. The rates

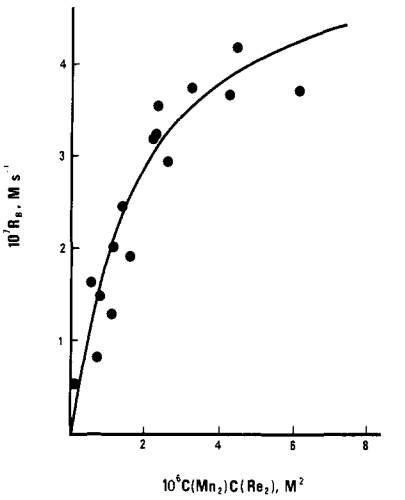

Figure 6. Dependence of R_B, the initial rate of reaction under N_2 at 190 °C by path B, on $C(Mn_2)C(Re_2)$. The continuous line is drawn according to least-squares parameters obtained from the plot in Figure 7.

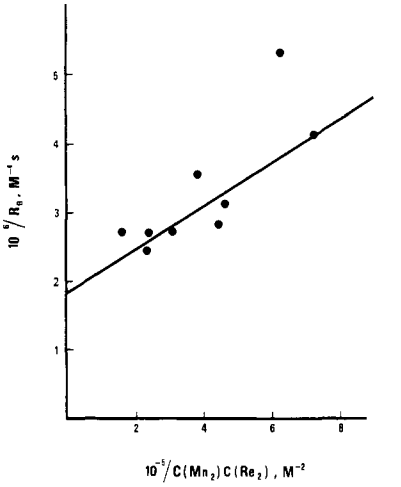

Figure 7. Dependence of $1/R_B$ on $1/C(Mn_2)C(Re_2)$ for reaction by path B at 190 °C under N_2. The line drawn is based on a weighted least-squares analysis and corresponds to $\sigma(R_B) = \pm 14\%$.

of the major path (path A) are closely linear in the product $C(Mn_2)C(Re_2)$ (eq 3) and, at 170 and 180 °C, the reactions are retarded by the presence of free CO according to eq 4. An

$$R_A = k_2 C(Mn_2)C(Re_2) \quad (3)$$

$$k_2 = p/\{1 + qp(CO)^3\} \quad (4)$$

important feature of Figure 3 is that it shows that $qp(CO)^3$ varies from being $\ll 1$ to ca. 4. The minor path (path B) is important mainly at 190 °C, and reaction by this path shows the unusual feature of increasing in rate with increasing $C(Mn_2)C(Re_2)$ until a limiting rate, independent of this product, is reached. This limiting rate is inversely proportional to $p(CO)^2$ (Figure 5). Both paths must therefore involve stepwise and reversible loss of a small number of CO ligands and aggregation of two dinuclear species. The question then arises as to whether some or all of the CO ligands are lost from the separate dinuclear complexes before aggregation or whether reversible aggregation occurs first, followed by stepwise and reversible CO loss. Since there are two paths it might be hypothesized that one path involves the extreme of dissociative loss of all the required number of CO ligands before aggregation while the other path involves the extreme of aggregation before any CO dissociation occurs. It turns out that the kinetic data for path A can only be consistently explained by the *latter* alternative. This conclusion rests on the fact that, if there is *any* reversible CO loss before aggregation, steady state analysis

can lead to a rate equation such as (3) only when k_2 is inversely proportional to some power of $p(CO)$, e.g., in eq 4, $qp(CO)^3 \gg 1$. The significant intercepts in Figures 3 and 4 show clearly that this is not the case and that the data for path A are therefore qualitatively quite inconsistent with there being any CO dissociation before aggregation. On the other hand, the data can be qualitatively and quantitatively accounted for according to initial aggregation followed by a sequence of CO dissociative steps as shown in Scheme I.

Equations 3 and 4 require that $Mn_2Re_2(CO)_{17}$ must be formed as a reactive intermediate or, possibly, a transition state. It is convenient, however, to discuss the mechanism initially in terms of the reaction's passing through the reactive intermediate $Mn_2Re_2(CO)_{16}$. $Mn_4(CO)_{16}$[11] has been isolated and characterized by mass spectroscopy and $[Re(CO)_4]_n$[12] (n believed to be 4) has also been isolated. Little is known about their chemical properties and structures although it appears that neither contains any bridging carbonyls. Attempts to prepare $Re_4(CO)_{16}$ under the conditions of the kinetic experiments failed and suggest that, if formed, $Mn_2Re_2(CO)_{16}$ is likely to be only a reactive intermediate present in undetectable concentrations during the reactions studied here. Any $Mn_4(CO)_{16}$ and $Re_4(CO)_{16}$ formed in similarly low concentrations during the reactions would not lead to any scrambling and would be unimportant "cul-de-sac reactions" without any effect on the kinetics. In order to reach $Mn_2Re_2(CO)_{16}$ or $Mn_2Re_2(CO)_{17}$ via initial reversible aggregation a sequence of reactions involving stepwise loss of CO from $Mn_2Re_2(CO)_{20}$ has to occur. No reversible single-step formation of $Mn_2Re_2(CO)_{16}$ from $Mn_2(CO)_{10}$ and $Re_2(CO)_{10}$ is conceivable.

The essential features of the proposed scheme therefore involve initial reversible aggregation of $Mn_2(CO)_{10}$ and $Re_2(CO)_{10}$ to form a tetranuclear complex $Mn_2Re_2(CO)_{20}$, Ia. This can be envisaged for simplicity as consisting of a quasitetrahedral cluster of metal atoms that contains one Mn–Mn and one Re–Re bond. The remaining four edges of the tetrahedron comprise metal atoms held together by bridging carbonyl groups without any direct metal–metal interaction. These are represented by the dotted lines in Scheme I. Each metal atom also has four terminally bonded CO ligands and is therefore formally consistent with the 18-electron rule. These terminal CO ligands are omitted from Scheme I for the sake of clarity. Formation of Ia is followed by a succession of reversible CO dissociative processes, each one of which involves loss of a bridging CO and its replacement by a Mn–Re bond or, in the reverse reaction, insertion of a CO into the Mn–Re bond. The number of terminal CO groups remains constant and the 18-electron rule is adhered to by all the proposed intermediates. These processes lead eventually to $Mn_2Re_2(CO)_{16}$ (V) which contains six metal–metal bonds, no bridging CO groups, and four terminal CO groups on the metal atoms, each of which also formally adheres to the 18-electron rule. When $Mn_2Re_2(CO)_{19}$ (in the form shown by IIa) loses a bridging CO it can, in principle, do it in three ways to form the three isomeric forms of $Mn_2Re_2(CO)_{18}$ shown as IIIa, IIIb, and IIIc. Each of these can only form the isomer IVa on loss of a bridging CO. Having reached $Mn_2Re_2(CO)_{16}$ the system can then undergo a different series of additions of CO in which metal–metal bonds are replaced by bridging CO groups. In order to end up with the scrambled product, $MnRe(CO)_{10}$, this sequence has to begin with insertion of CO into the Mn–Mn and Re–Re bonds of V so that the isomer, Ib, of $Mn_2Re_2(CO)_{20}$ is eventually formed. Fragmentation of Ib will form two $MnRe(CO)_{10}$ molecules. Just as at least four intermediates must be involved in the stepwise formation of $Mn_2Re_2(CO)_{16}$ from $Mn_2(CO)_{10}$ and $Re_2(CO)_{10}$, so a similar number must be involved in the formation of $MnRe(CO)_{10}$ from $Mn_2Re_2(CO)_{16}$. The clusters I–IV, including all the isomeric forms, are envisaged as being highly reactive intermediates, present only in negligible concentrations, and their formulation is not intrinsically improbable.[13]

Scheme I

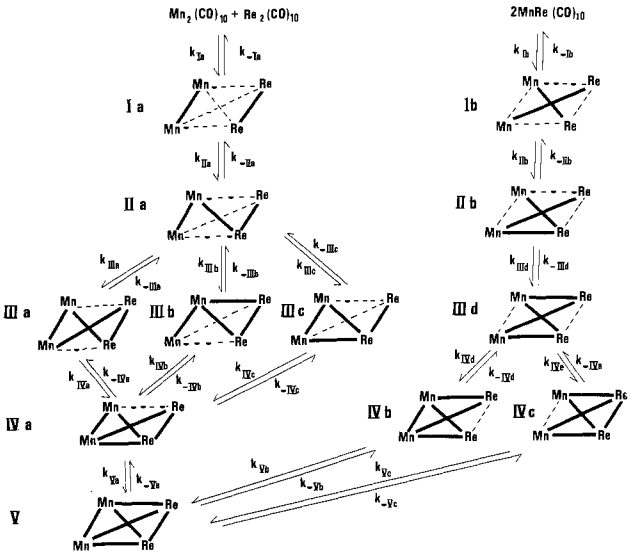

The scheme can be related to the empirical rate equation in several closely related ways. The simplest is to regard the clusters Ia, IIa, IIIa, IIIb, IIIc, and IVa as being in labile equilibrium with each other, and to regard the formation of IVb and IVc from V as essentially irreversible, i.e., $k_{-Vb}[CO] \gg k_{Vb}$, etc. This leads to the rate equation shown in eq 5. Since $[CO] \propto p(CO)$, this

$$k_2 = k_{Ia}/\{1 + k_{-Ia}(k_{-Va} + k_{-Vb} + k_{-Vc}) \times [CO]^3/K_{IIa}K_{IIIa}K_{IVa}K_{Va}(k_{-Vb} + k_{-Vc})\} \quad (5)$$

has exactly the form of eq 4 and the scheme can be represented by the energy profile shown diagrammatically in Figure 8. The barriers in the profile are a reflexion of the rates of reaction (not rate constants) and can therefore be concentration dependent. The profile as drawn corresponds to relatively low values of [CO]. As [CO] becomes larger, so the energies of the intermediates to the right will rise compared with those to the left and vice versa. This is because the reactions of each of the intermediates IIa–V to form the intermediate lying to its left are first order in [CO] and the barriers for movement to the left will decrease with increasing [CO]. Movement to the right is simply first order in the various intermediates and independent of [CO]. The height of the barriers for movement from left to right therefore remains constant, irrespective of [CO]. The relative heights of the two barriers for reaction of V to IVa or to IVb and IVc will also be independent of [CO] because reaction in both directions is first order in [CO] and the relative rates are therefore independent of [CO]. It is because of this that it is not possible to distinguish between the case where IVa converts to IVb and IVc directly or via V as is indicated in Scheme I. If the former is the preferred path (and

(11) Jaintner, P. E.; Schwartzhaus, K. E. *Z. Naturforsch., B* **1977**, *32B*, 705.

(12) Osborne, A. G.; Stiddard, M. H. B. *J. Organomet. Chem.* **1965**, *3*, 340.

(13) Similar intermediates have been invoked to explain the kinetics of the [CO]-dependent reaction of $Co_4(CO)_{12}$ to form $Co_2(CO)_8$ via species such as $Co_4(CO)_{13}$.[14] Many other clusters that are no less improbable in our view have been isolated and characterized by crystalography![15] The proposed existence of reactive intermediates containing pairs of metal atoms bridged by CO ligands without any direct metal–metal bonding has quite a long history[16] and is currently accepted[17] as a useful or necessary hypothesis in explaining kinetic features of several reactions. Complexes believed to contain such bridges have also been characterized spectroscopically.[18]

(14) Bor, G.; Dietler, U. K.; Pino, P.; Poë, A. J. *J. Organomet. Chem.* **1978**, *154*, 301.

(15) E.g., the butterfly structure of $HFe_4(CO)_{13}$ with the η^2-CO ligand: Monassero, M.; Sansoni, M.; Longini, G. *J. Chem. Soc., Chem. Commun.* **1976**, 919.

(16) Breitschaft, S.; Basolo, F. *J. Am. Chem. Soc.* **1966**, *88*, 2702. Barrett, P. F.; Poë, A. J. *J. Chem. Soc. A*, **1968**, 429.

(17) Poë, A. J. In "Reactivity of Metal–Metal Bonds"; Chisholm, M. H., Ed.; American Chemical Society: Washington, DC; ACS Symp. Ser. No. 155, p 147. Malito, J.; Markiewicz, S.; Poë, A. J. *Inorg. Chem.*, **1982**, *21*, 4335. Desrosiers, M. F.; Ford, P. C. *Organometallics* **1982**, *1*, 1715. Stiegman, A. E.; Tyler, D. R. *J. Am. Chem. Soc.* **1982**, *104*, 2944.

(18) Tyler, D. R.; Schmidt, M. A.; Gray, H. B. *J. Am. Chem. Soc.* **1979**, *101*, 2753.

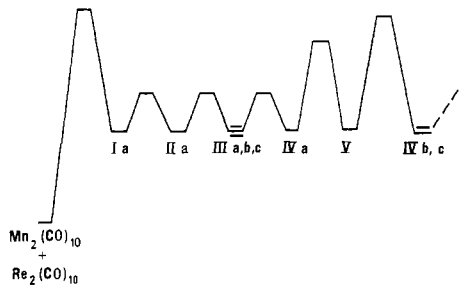

Figure 8. Diagrammatic representation of the energy profile corresponding to the formation of $Mn_2Re_2(CO)_{16}$ in Scheme I. The intermediates Ia to IVa are taken to be in labile equilibrium so that the barriers between them are low. Higher barriers would imply that they were steady state intermediates. The equality of energies assigned to Ia–V is arbitrary and, as [CO] increases, energies will increase steadily from Ia to V and vice versa. The relative heights of the first and last barriers are also arbitrary and under some conditions the height of the first barrier can be rate determining.

is governed by rate constants k'_{-IVb} and k'_{-IVc} for direct formation of IVb and IVc, respectively) then $k_{Va}(k_{-Vb} + k_{-Vc})/(k_{-Va} + k_{-Vb} + k_{-Vc})$ in eq 5 should be replaced by $(k'_{-IVb} + k'_{-IVc})$. It must be noted that the species in labile equilibrium with each other in the left-hand column of Scheme I cannot also be in labile equilibrium with any of their respective isomers in the series of reactions by which Ib is formed from V in the right-hand column. If, for instance, Ia and Ib were in labile equilibrium the rates would not depend on [CO] at all.

An alternative way of relating the scheme to eq 4 is to regard all the species from Ia to Va to be in steady state equilibria. Again, k_{-Vb}[CO] is assumed to be much greater than k_{Vb}, etc. The rate is then governed by eq 6. This equation[19] can correspond to the

$$k_2 = k_{Ia}/\left\{1 + \frac{k_{-Ia}}{k_{IIa}} + \frac{k_{-Ia}k_{-IIa}[CO]}{k_{IIa}k^*_{IIIa}} + \frac{k_{-Ia}k_{-IIa}k_{-IIIa}}{k_{IIa}k^*_{IIIa}k_{IVa}}[CO]^2 + \frac{k_{-Ia}k_{-IIa}k_{-IIIa}k^*_{-IVa}}{k_{IIa}k^*_{IIIa}k_{IVa}k_{Va}}\frac{(k_{-Va} + k_{-Vb} + k_{-Vc})}{(k_{-Vb} + k_{-Vc})}[CO]^3\right\} \quad (6)$$

empirical rate behavior provided certain inequalities are fulfilled, e.g., $k^*_{-IVa}[CO] \gg k_{Va}(k_{-Vb} + k_{-Vc})/(k_{-Va} + k_{-Vb} + k_{-Vc})$. On the other hand, $k_{-Ia}k_{-IIa}[CO]/k_{IIa}k^*_{IIIa}$ must be $\ll 1 + k_{-Ia}/k_{IIa}$ for there to be an intercept in the plot of $1/k_2$ against $p(CO)^3$ as in Figure 3. There seems to be no reason why such inequalities should not be operative and this way of describing the scheme differs from that reflected in eq 5 only in regard to the relative energies of some of the peaks and valleys in the energy profile in Figure 8.

When the reaction occurs at 190 °C, $1/k_2$ depends linearly on $p(CO)^2$ and/or $p(CO)$ rather than $p(CO)^3$ as at the lower temperatures. An important factor contributing to this may be the pronounced decrease in the values of [CO] corresponding to particular values of $p(CO)$. This occurs because of the rapid rise of the vapor pressure of the solvent over this temperature range.[20] The term in $[CO]^3$ in eq 6 will therefore be relatively less important at 190 °C compared with those in $[CO]^2$ and [CO]. This trend could be reinforced if the inequality $\Delta H^{\ddagger}_{Va} > \Delta H^{\ddagger}_{-IVa}$ applies. In terms of the labile equilibrium model the decrease in [CO] would decrease the relative amounts of IIIa, IIIb, and IIIc in equilibrium with IVa. However, if this were more than compensated for by a growing importance of direct conversion of IIIa, IIIb, and IIIc to IIId, then the lower dependence on $p(CO)$ at 190 °C could be accounted for. Direct conversion of IVa to IVb and IVc was acknowledged above to be perfectly consistent with the data at 170 and 180 °C, and conversion of IIIa, etc., to IIId might well become of importance at the higher temperature. If this explanation is taken to be unsatisfactory, then the steady state model becomes more favored.

All the essential features of the kinetic behavior characteristic of path A are, therefore, readily accounted for in terms of one or another of these slightly different versions of Scheme I. On the basis of the quite extensive kinetic data, we find it difficult to picture any significantly different scheme that would be as satisfactory.

The temperature dependence of the inverse of the intercepts in Figures 3 and 4 leads to the values $\Delta H^{\ddagger} = 22 \pm 3$ kcal mol^{-1} and $\Delta S^{\ddagger} = -20 \pm 6$ cal K^{-1} mol^{-1}, the uncertainties corresponding to an estimated uncertainty of ±10% in the intercepts. These parameters correspond either to $\Delta H^{\ddagger}_{Ia}$ and $\Delta S^{\ddagger}_{Ia}$ (eq 5, or eq 6 with $k_{-Ia} \ll k_{IIa}$) or $\Delta H^{\circ}_{Ia} + \Delta H^{\ddagger}_{IIa}$ and $\Delta S^{\circ}_{Ia} + \Delta S^{\ddagger}_{IIa}$ (eq 6, $k_{-Ia} \gg k_{IIa}$), respectively, or to some less-well-defined intermediate between these two. It is worth noting that the former alternative implies that, at low values of $p(CO)$, the rate-determining step is simple aggregation of the two decacarbonyls and no CO dissociation is then involved in that step. The details of this aggregation are not easy to envisage precisely. Presumably the sets of ligands on each metal have to be distorted away from each other to make room for the approach of the other molecule, but no very extensive bond breaking would have to occur. The overall process of aggregation could well be relatively neutral in terms of changes in the sum of *bonding* interactions since the strength of bonding of a bridging CO is about the same as that of a terminal CO.[21] The increase of enthalpy associated with aggregation would result mainly from increased ligand–ligand repulsion, but this need not be unreasonably large since 7-coordinate complexes of the first-row elements are, of course, well known.[22] The value of $\Delta S^{\ddagger}$ is not as negative as might have been expected for the aggregation above, and it may seem more likely that the −20 cal K^{-1} mol^{-1} would be made of a more negative value for ΔS°_{Ia} (say −40 cal K^{-1} mol^{-1}) offset by a positive value (e.g., +20 cal K^{-1} mol^{-1}) for the CO dissociative path governed by $\Delta S^{\ddagger}_{IIa}$. The transition state defined by the observed $\Delta H^{\ddagger}$ and $\Delta S^{\ddagger}$ is therefore more likely to correspond to the barrier between Ia and IIa rather than that between the separate decacarbonyls and Ia as implied in Figure 8. This does not have any significant effect on the form of the kinetics.

At 190 °C the other path (path B) is predominant at lower concentrations of complex and lower values of $p(CO)$. The data conform quite well with eq 7 as shown by Figures 5, 6, and 7 (r and s are constants). The limiting rates, $r/sp(CO)^2$, at high values

$$R_B = rC(Mn_2)C(Re_2)/\{1 + sC(Mn_2)C(Re_2)p(CO)^2\} \quad (7)$$

of $C(Mn_2)C(Re_2)$ are provided by k_0 (Table I). The value of (5.9 ± 1.7) × 10^{-7} M s^{-1} obtained from the intercept in Figure 7 is in good agreement with the value of k_0 (Table I) found from reactions carried out under similar conditions. The values of k_0 are inversely proportional to $p(CO)^2$ in accord with eq 7.

The most difficult aspect of these data is the approach to a limiting rate with increasing $C(Mn_2)C(Re_2)$. Since we have proposed initial aggregation followed by stepwise CO dissociation for path A, it follows that path B must involve initial CO dissociative steps before aggregation. Reactions 8–12 in Scheme II can therefore be suggested as a possible sequence of reactions that leads to scrambling via $Mn_2Re_2(CO)_{16}$.[23] This can lead to

(19) $k^*_{IIIa} = \alpha k_{IIIa}$ and $k^*_{-IVa} = \alpha k_{-IVa}$. α is a term that accounts for the splitting of the reaction path into three parallel paths before converging again to a single path. It takes the form $1 + \{k_{IIIb}(1 + k_{-IIIa}/k_{IVa})/k_{IIIa}(1 + k_{-IIIb}/k_{IVb})\} + \{k_{IIIc}(1 + k_{-IIIa}/k_{IVa})/k_{IIIa}(1 + k_{-IIIc}/k_{IVc})\}$. Clearly when k^*_{-IVa}/k^*_{IIIa} occurs in a term the constant α cancels and the ratio can be replaced by k_{-IVa}/k_{IIIa}. It is only the two terms that contain k^*_{IIIa}, but not k^*_{-IVa} as well, that are affected by the value of α.

(20) Weast, R. C., Ed. "Handbook of Chemistry and Physics"; The Chemical Rubber Co.: Cleveland, Ohio, 1972.

(21) Connor, J. A. *Top. Curr. Chem.* **1977**, *71*, 71.

(22) Cotton, F. A.; Wilkinson, G. "Advanced Inorganic Chemistry"; Wiley: New York; 4th ed, 1980.

(23) Reaction 8 has to be regarded as a labile equilibrium since the half-lives for reaction of $Mn_2(CO)_{10}$ at 170, 180, and 190 °C can be calculated by extrapolation of data for lower temperatures[24] to be 16, 6, and 2.5 s, respectively. Those for $Re_2(CO)_{10}$ are much longer, viz., 14, 5, and 2 min, respectively.[25]

(24) Jackson, R. A.; Poë, A. J. *Inorg. Chem.* **1978**, *17*, 997.

(25) Fawcett, J. P.; Poë, A. J. *J. Chem. Soc., Dalton Trans.* **1976**, 2039.

Scheme II

$$Mn_2(CO)_{10} \overset{K_8}{\rightleftharpoons} Mn_2(CO)_9 + CO \quad (8)$$

$$Mn_2(CO)_9 \underset{k_{-9}}{\overset{k_9}{\rightleftharpoons}} Mn_2(CO)_8 + CO \quad (9)$$

$$Re_2(CO)_{10} \underset{k_{-10}}{\overset{k_{10}}{\rightleftharpoons}} Re_2(CO)_9 + CO \quad (10)$$

$$Re_2(CO)_9 \underset{k_{-11}}{\overset{k_{11}}{\rightleftharpoons}} Re_2(CO)_8 + CO \quad (11)$$

$$Mn_2(CO)_8 + Re_2(CO)_8 \xrightarrow{k_{12}} Mn_2Re_2(CO)_{16} \quad (12)$$

$$Mn_2Re_2(CO)_{16} + CO \rightarrow IVa + IVb + IVc \text{ and/or } MnRe(CO)_8 \quad (13)$$

$$Mn_2(CO)_8 + Re_2(CO)_{10} \xrightarrow{k_{14}} Mn_2Re_2(CO)_{18} \quad (14)$$

$$Re_2(CO)_8 + Mn_2(CO)_{10} \xrightarrow{k_{15}} Mn_2Re_2(CO)_{18} \quad (15)$$

$MnRe(CO)_{10}$ either by fragmentation to $MnRe(CO)_8$ (followed by CO uptake) or via formation of Vb and Vc as in Scheme I. These reactions by themselves would not result in a limiting rate at high $C(Mn_2)C(Re_2)$, and we find it necessary to postulate reactions 14 and 15 in order to account for this. These reactions reduce the concentrations of $Mn_2(CO)_8$ and $Re_2(CO)_8$ involved in reaction 12.[26]

Under conditions such that $k_{14}C(Re_2) \gg k_{-9}[CO] + k_{12}[Re_2(CO)_8]$, $k_{15}C(Mn_2) \gg k_{-11}[CO] + k_{12}[Mn_2(CO)_8]$, and $k_{-10}[CO] \gg k_{11}$, scrambling via reactions 12 and 13 should proceed at rates governed by eq 16, which gives the rate, R_B', of formation

$$R_B' = \{K_8k_9k_{10}k_{11}k_{12}/k_{-10}k_{14}k_{15}[CO]^2\} \quad (16)$$

of $Mn_2Re_2(CO)_{16}$ via path B. On the other hand, at lower values of $C(Mn_2)$ and $C(Re_2)$ (and provided $k_{12}[Re_2(CO)_8] \ll k_{-9}[CO]$, $k_{12}[Mn_2(CO)_8] \ll k_{-11}[CO]$, and $k_{-10}[CO] \gg k_{11}$) the rate equation at constant [CO] takes the form shown in eq 17.[27] At

$$R_B' = cC(Mn_2)C(Re_2)/\{1 + dC(Mn_2) + eC(Re_2) + fC(Mn_2)C(Re_2)\} \quad (17)$$

very low values of $C(Mn_2)$ and $C(Re_2)$ R_B' is given by $cC(Mn_2)C(Re_2)$. It is therefore possible to explain the increase in the rate of path B from an initial linear dependence on $C(Mn_2)C(Re_2)$ at low concentrations of complex to a limiting value independent of concentrations of complex and inversely dependent on $p(CO)^2$ at high concentrations.[28]

Most of the data used in Figure 7 for reactions under N_2 were obtained with a constant value of $C(Mn_2)$ so that the concentration of CO was controlled at a reasonably constant value by the equilibrium in reaction 8. The scatter shown by the data in Figure 6 at lower values of $C(Mn_2)C(Re_2)$ can be ascribed to variable values of $C(Mn_2)$ and consequently variable concentrations of CO. Indeed the higher values of R_B correspond to lower values of $C(Mn_2)$ and vice versa, as expected. The rather complex scheme proposed accounts very well qualitatively and fairly well quantitatively for all the observed data in a way not accomplished by any readily obvious and more simple alternative.

Although scrambling via reactions 12 and 13 at high $C(Mn_2)$ and $C(Re_2)$ proceeds at a constant rate due to the intervention of reactions 14 and 15, the discussion of path A above shows that scrambling should also occur by further reaction of the $Mn_2Re_2(CO)_{18}$ formed by these reactions. The maximum relative importance of this extra contribution can be shown to depend on the sum of two terms, one inversely proportional to $C(Mn_2)p(CO)$ and the other to $C(Re_2)p(CO)$. This could enhance the rates at 190 °C and high concentrations that were previously attributed only to path A. However, Figure 4 suggests that this contribution is probably only significant for reactions proceeding at low values of $p(CO)$. This would explain the anomalously low value of $1/k_2$ found when $p(CO) = 0$. The intercept of the plot in Figure 4 would then still be a good measure of k_{Ia} or $k_{Ia}k_{IIa}/k_{-Ia}$ (see above), and it does, indeed, lie on a good Eyring plot based on the intercepts in Figures 3 and 4. In any case, the extra contribution to the rates at higher values of $C(Mn_2)$ and $C(Re_2)$ will be important only at 190 °C whereas at 180 °C and, even more, at 170 °C (where there is much less contribution by path B to the rates) this complication should not be important.

Summary and Conclusions

The kinetics suggest that the scrambling reaction between $Mn_2(CO)_{10}$ and $Re_2(CO)_{10}$ proceeds cleanly by two paths, both of which involve aggregation to form tetranuclear clusters as reactive intermediates. These clusters can all conform to the 18-electron rule by having four terminal carbonyls on each metal atom, $4 - n$ carbonyls bridging two metal atoms without any metal–metal bonding, and $n + 2$ pairs of metal atoms joined only by metal–metal bonds ($n \leq 4$).

The two paths are distinguished by whether CO dissociation occurs before or after aggregation to form the Mn_2Re_2 clusters. The more facile path occurs over the whole range of temperatures and values of $p(CO)$ used in this study and involves aggregation before any loss of CO. This is followed by successive dissociation of up to four CO ligands. The clusters involved in these steps all have one Mn–Mn and one Re–Re bond together with increasing numbers of Mn–Re bonds. Eventually, one or another of these intermediates undergoes reaction whereby the Mn–Mn and Re–Re bonds are lost. This can occur either by insertion of a CO ligand or by isomerization involving redistribution of the metal–metal and bridging CO bonds in the clusters. Subsequent insertion of more CO groups leads to the isomer of $Mn_2Re_2(CO)_{20}$ that contains only two metal–metal bonds, both Mn–Re. This undergoes very ready fragmentation to form two $MnRe(CO)_{10}$ molecules.

The minor path is of relative importance only at 190 °C and at lower concentrations of the complexes and lower values of $p(CO)$. It involves loss of two CO ligands from each decacarbonyl before aggregation[29] to $Mn_2Re_2(CO)_{16}$. This path is much more severely retarded by CO than the other. This can probably be accounted for in simple terms by the idea that each loss of CO from the dinuclear carbonyls can be compensated for only by the formation of a "sideways on" CO–metal bond, as in VI and VII, or by formation of metal–metal π bonds as in VIII and IX. This contrasts with loss of the bridging CO ligands from the tetranuclear complexes which is accompanied by formation of a metal–metal σ bond.

It is interesting that the mechanisms followed involve exactly the opposite process (aggregation) to the one we would have predicted (homolytic fragmentation).[2,3] Extension[31] of earlier studies[3] of reactions of $Re_2(CO)_{10}$ has confirmed that the rate of reaction with O_2 does decrease with the concentration of

(26) If scrambling were to occur by combination of $Mn_2(CO)_9$ and $Re_2(CO)_9$, limiting rates would not be observed even if these intermediates were individually scavenged by $Re_2(CO)_{10}$ and $Mn_2(CO)_{10}$, respectively. In this case the rates increase to become independent of $C(Mn_2)$ but remain first order in $C(Re_2)$.

(27) $c = K_8k_9k_{10}k_{11}k_{12}/k_{-9}k_{-10}k_{-11}[CO]^4$, $d = k_{15}/k_{-11}[CO]$, $e = k_{14}/k_{-9}[CO]$, and $f = k_{14}k_{15}/k_{-9}k_{-11}[CO]^2$. NB.: eq 16 and 17 illustrate the fact that, when CO dissociation precedes aggregation, the rates cannot follow eq 3 and 4 at the same time.

(28) It turns out that it is not possible for the terms $dC(Mn_2)$ and $e(Re_2)$ in eq 17 to be simultaneously much less than $fC(Mn_2)C(Re_2)$ and much greater than 1 so the simple form of the curvature of R_B with increasing $C(Mn_2)C(Re_2)$ as shown by eq 7 and Figures 6 and 7 is probably fortuitous.

(29) A similar reversible loss of two CO ligands is believed[30] to occur prior to the aggregation of two $Co_2(CO)_6$ intermediates to form $Co_4(CO)_{12}$ from $Co_2(CO)_8$.

(30) Ungváry, F.; Markó, L. *Inorg. Chim. Acta* **1970**, *4*, 324.

(31) Marcomini, A.; Poë, A. J., unpublished observations.

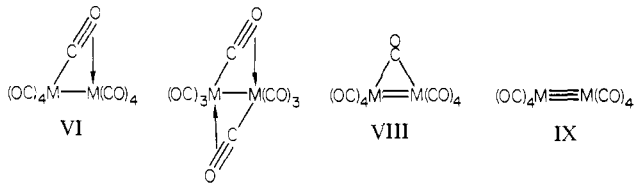

VI VII VIII IX

complex and has also revealed that reaction with $C_{16}H_{33}I$ to form $Re(CO)_5I$ shows similar kinetic behavior to that previously taken[3] to imply reversible homolytic fission. The experimental facts remain, therefore, very similar, but their interpretation requires re-evaluation and extension.

Acknowledgment. We thank the Natural Sciences and Engineering Research Council, Ottawa, for support and Professors Basolo and Trogler, and Professor Muetterties, for communicating their results to us before publication.

Appendix

Derivation of Rate Equations. Equation 5 is derived simply by regarding the intermediates Ia–IVa in Scheme I as a single steady state assemblage. The rate of formation of this is given by $k_{Ia}C(Mn_2)C(Re_2)$ and equals its rate of loss which is given by $k_{-Ia}[Ia] + xk_{Va}[IVa]$, where $x = (k_{-Vb} + k_{-Vc})/(k_{-Va} + k_{-Vb} + k_{-Vc})$. Since $[Ia] = [IVa][CO]^3/K_{IIa}K_{IIIa}K_{IVa}$, and the rate is given by $xk_{Va}[IVa]$, eq 5 follows.

The derivation of eq 6 is more complicated and a derivation for a somewhat simplified model will be given. Consider the following scheme.

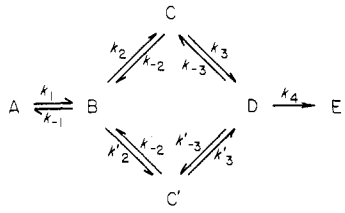

$R = -d[A]/dt = k_1[A] - k_{-1}[B] = k_4[D]$
$[B] = (R_1 - R)/k_{-1}$ when $R_1 = k_1[A]$
$d[B]/dt = R - (k_2 + k_2')[B] + k_{-2}[C] + k_{-2}'[C'] = 0$
$d[C]/dt = k_2[B] - (k_{-2} + k_3)[C] + k_{-3}[D] = 0$
$d[C']/dt = k_2'[B] - (k_{-2}' + k_3')[C'] + k_{-3}'[D] = 0$
$d[D]/dt = k_3[C] + k_3'[C'] - (k_{-3} + k_{-3}')[D] - R = 0$
$[C] = (k_2[B] + k_{-3}[D])/(k_{-2} + k_3)$
$[C'] = (k_2'[B] + k_{-3}'[D])/(k_{-2}' + k_3')$
$(k_{-3} + k_{-3}')[D] = k_3[C] + k_3'[C'] - R =$

$$\left[\frac{k_2k_3}{k_{-2}+k_3} + \frac{k_2'k_3'}{k_{-2}'+k_3'}\right]\left[\frac{R_1-R}{k_{-1}}\right] + \left[\frac{k_3k_{-3}}{k_{-2}+k_3} + \frac{k_3'k_{-3}'}{k_{-2}'+k_3'}\right][D] - R$$

Collecting terms in [D] and taking $R = k_4[D]$:

$$R = \frac{k_2k_3k_4}{k_{-1}k_{-2}k_{-3}}\frac{(1+\alpha)(R_1-R)}{(1+\beta)} - \frac{k_4(k_{-2}+k_3)R}{k_{-2}k_{-3}(1+\beta)}$$

where $\alpha = 1 + (k'_2k_3'/k_2k_3)(k_{-2} + k_3)/(k_{-2}' + k_3')$ and $\beta = 1 + (k_{-2}'k_{-3}'/k_{-2}k_{-3})(k_{-2} + k_3)/(k_{-2}' + k_3')$. But $k_2k_3/k_{-2}k_{-3} = k_2'k_3'/k_{-2}'k_{-3}'$, whence $\alpha = \beta = 1 + k_2'(1 + k_{-2}/k_3)/k_2(1 + k_{-2}'/k_3')$ and $R = k_1[A]/\{1 + k_{-1}/k_2^* + k_{-1}k_{-2}/k_2^*k_3 + k_{-1}k_{-2}k_{-3}^*/k_2^*k_3k_4\}$, where $k_2^* = k_2\alpha$ and $k_{-3}^* = k_{-3}\alpha$. If there is an additional intermediate, C'', formed from B the rate equation remains unchanged except that α becomes $1 + k_2'(1 + k_{-2}/k_3)/k_2(1 + k_{-2}'/k_3') + k_2''(1 + k_{-2}/k_3)/k_2(1 + k_{-2}''/k_3'')$. Equation 6 can be obtained by a similar though more lengthy derivation. Indeed, the same procedure can be extended so as to include all the steps through to formation of Ib. The resulting equation has exactly the same form as eq 6 but the constants involved are, of course, different. However, we consider it more realistic to assume that addition of CO to the tetrahedral clusters (particularly $Mn_2Re_2(CO)_{16}$) is generally more rapid than their formation by loss of CO. $k_{-Vb}[CO]$ is therefore much greater than k_{Vb}, etc., which is the basis on which eq 6 is derived.

Derivation of eq 16 and 17 is quite straightforward. $[Mn_2(CO)_8]$ and $[Re_2(CO)_8]$ are as shown below but are not easily solved

$$[Mn_2(CO)_8] = \{K_8k_9C(Mn_2)/[CO]\}/\{k_{-9}[CO] + k_{12}[Re_2(CO)_8] + k_{14}C(Re_2)\}$$

$$[Re_2(CO)_8] = \{k_{10}k_{11}C(Re_2)/(k_{-10}[CO] + k_{11})\}/\{k_{-11}[CO] + k_{12}[Mn_2(CO)_8] + k_{15}\,C(Mn_2)\}$$

for unless the terms $k_{12}[Re_2(CO)_8]$ and $k_{12}[Mn_2(CO)_8]$ are both relatively quite small. Since the rate of reaction is proportional to $k_{12}[Mn_2(CO)_8][Re_2(CO)_8]$, eq 16 is obtained when $k_{13}C(Re_2)$ and $k_{14}C(Mn_2)$ are dominant terms in the denominators, while eq 17 is obtained directly provided the terms $k_{12}[Re_2(CO)_8]$, $k_{12}[Mn_2(CO)_8]$, and k_{11} are negligible.

Registry No. $Mn_2(CO)_{10}$, 10170-69-1; $Re_2(CO)_{10}$, 14285-68-8; $MnRe(CO)_{10}$, 14693-30-2.

Supplementary Material Available: Tables of kinetic data (3 pages). Ordering information is given on any current masthead page.